Supersymmetric corrections to heavy quark pair production in e^+e^- annihilation

Chao-Hsi Chang,[1,2] Chong Sheng Li,[1,2,3] R. J. Oakes,[4] and Jin Min Yang[1,2]
[1] *Chinese Center of Advanced Science and Technology (World Laboratory), P.O. Box 8730, Beijing 100080, People's Republic of China*
[2] *Institute of Theoretical Physics, Academia Sinica, Beijing 100080, People's Republic of China**
[3] *Department of Physics, Chongqing University, Chongqing, Sichuan 630044, People's Republic of China**
[4] *Department of Physics and Astronomy, Northwestern University, Evanston, Illinois 60208*
(Received 14 July 1994; revised manuscript received 31 October 1994)

The supersymmetric $O(\alpha m_t^2/m_W^2)$ corrections to $t\bar{t}$ and $b\bar{b}$ production in e^+e^- annihilation are calculated in the minimal supersymmetric model. We consider the polarization of the electron beam and present the analytic expression for the renormalized differential cross section in terms of the well-known notation of Feynman integrals. We find that the corrections to the total cross section and the left-right asymmetry can both reach a few percent for favorable parameter values, but for the forward-backward asymmetry the correction is negligibly small (<1%).

PACS number(s): 13.65.+i, 12.15.Lk, 12.38.Bx, 12.60.Jv

I. INTRODUCTION

The remarkable experimental success of the standard model (SM) has shown that new physics beyond the SM does not exist below the electroweak scale. Nevertheless, there are a number of unsolved theoretical puzzles which suggest that new physics beyond the SM must exist at an energy scale of $\sim$ 1 TeV or below. Supersymmetry (SUSY) is at present a promising theoretical framework for physics beyond the SM. One interesting SUSY model is the minimal supersymmetric extension of the standard model (MSSM) [1]. To solve the gauge hierarchy problem, SUSY must be broken at energies of about 1 TeV, and thus the supersymmetric particles of the MSSM must be within the reach of the next generation of colliders. In recent years, a great deal of effort has been made to discover SUSY. Unfortunately, no direct signal for SUSY has been observed so far. Therefore it is tempting to search for SUSY through precision measurements, where the virtual effects of supersymmetric particles might alter the SM predictions.

Recently, the evidence for top quark production, with a mass of $174\pm10^{+13}_{-12}$ GeV, has been reported by the Collider Detector Collaboration at Fermilab (CDF) with an integrated luminosity of 19.3 pb^{-1} [2]. Of course, the discovery of the top quark will open a number of new and interesting issues, such as the precision measurement of the mass, width and Yukawa couplings of the top quark. But even with 1000 pb^{-1} of luminosity, the Fermilab Tevatron could determine the top mass to 5 GeV or better [3]. At the future multi-TeV proton colliders such as the CERN Large Hadron Collider (LHC), $t\bar{t}$ production will be enormously larger than the Tevatron rates, but the accuracy with which the top mass can be measured in proton colliders is limited to about 2–3 GeV [3]. Blondel *et al.* [4] have argued that one must know the top mass to 1 GeV to take full advantage of the constraints that precision electroweak measurements put on the Higgs boson and other massive particles which might contribute to electroweak loops. Beyond this, it would be wonderful to make a precision measurement of the basic parameter m_t to 0.3 GeV or better for looking for new physics beyond the SM by the loop processes which are sensitive to m_t. At the next-generation linear collider (NLC) operating at a center-of-mass energy of 500 GeV, the $e^+e^- \to t\bar{t}$ event rate would be around 10^4/yr, comparable with the Tevatron; however the events would be much cleaner and top parameters would be easier to extract. At the NLC a top mass measurement with statistical uncertainty 0.3 GeV from 10 fb^{-1} luminosity is expected [3] and it is possible to separately measure all of the various production and decay form factors of the top quark at the level of a few percent [5]. Thus the theoretical calculation of the radiative corrections to the production and decay of the top quark is of importance. On the other hand, since the bottom quark pair production at e^+e^- colliders can be measured with high accuracy, it is also important to calculate the radiative corrections to b quark production.

In the SM and two Higgs doublet models, the radiative corrections to top and bottom quark pair production processes $e^+e \to t\bar{t}$ and $e^+e^- \to b\bar{b}$ have been calculated by many authors [6–9]. For both processes, the dominant virtual effects of SUSY arise from SUSY QCD corrections and SUSY electroweak corrections of order $\alpha m_t^2/m_W^2$ due to a heavy top quark. Supersymmetric QCD corrections to both processes have already been calculated [10]. In this paper we present the calculation of the supersym-

*Mailing address.

metric $O(\alpha m_t^2/m_W^2)$ corrections.

For process $e^+e^- \to b\bar{b}$ with a center-of-mass energy on the Z resonance, the supersymmetric $O(\alpha m_t^2/m_W^2)$ corrections can be obtained from the corresponding results for $Z \to b\bar{b}$, which have been presented in Ref. [11]. We will present the calculation of the SUSY $O(\alpha m_t^2/m_W^2)$ corrections to $b\bar{b}$ production above the energies reached at the CERN e^+e^- collider LEP I, which arise from the loop effects of genuine supersymmetric particles as well as the charged Higgs bosons. Our calculation is different from the calculation in earlier works [11] which only emphasized the effects of SUSY on the $Zb\bar{b}$ vertex, and did not take into account the effects of SUSY on the $\gamma b\bar{b}$ vertex and the effects of the interference between the photon exchange and the Z exchange diagrams as well as the box diagram since they can be neglected for a c.m. system (c.m.s.) energy on the Z resonance. But for a c.m.s. energy above the Z resonance, all these contributions should be considered.

For the process $e^+e^- \to t\bar{t}$, since the additional Higgs contributions of the MSSM have already been calculated in Ref. [9], we will only present the calculation of the supersymmetric $O(\alpha m_t^2/m_W^2)$ corrections, which arise from the virtual effects of genuine supersymmetric particles (chargino, neutralino, sfermion), and do not recalculate the additional Higgs contributions of MSSM.

In Secs. II and III, we present the analytic results for $e^+e^- \to t\bar{t}$ and $e^+e^- \to b\bar{b}$, respectively. In Sec. IV, we present some numerical examples and discuss the implications of our results. In Appendix A and Appendix B we present the tedious expressions of the form factors and matrix elements squared for $t\bar{t}$ production process.

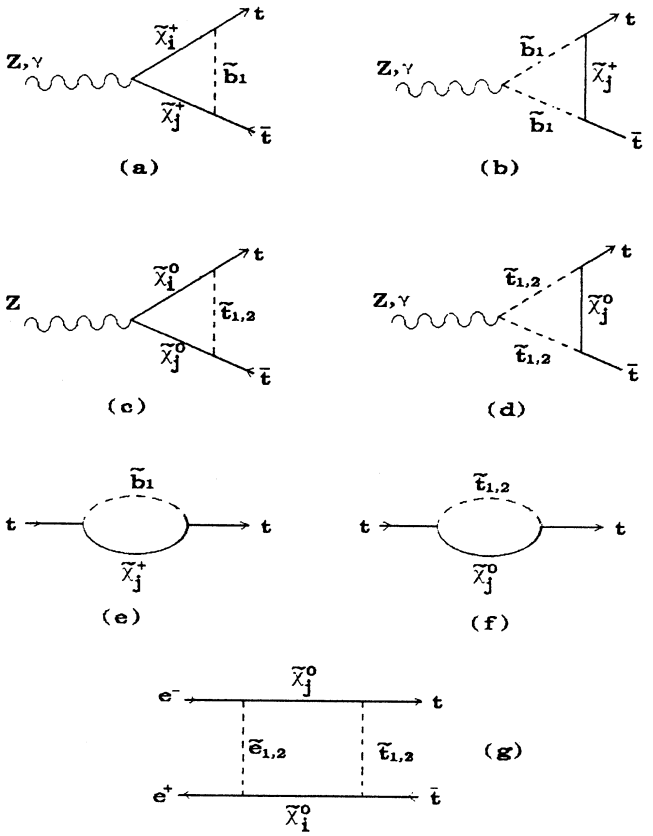

FIG. 1. Feynman diagrams contributing to $O(\alpha m_t^2/m_W^2)$ corrections to $e^+e^- \to t\bar{t}$: (a)–(d) vertex diagrams; (e) and (f) self-energy diagrams; (g) box diagrams. Here $\tilde{t}_i$, $\tilde{b}_i$, $\tilde{\chi}_j^+$, and $\tilde{\chi}_j^0$ stand for scalar top quark, scalar bottom quark, charginos, and neutralinos, respectively.

II. CALCULATIONS FOR $t\bar{t}$ PRODUCTION

The Feynman diagrams contributing to the genuine SUSY $O(\alpha m_t^2/m_W^2)$ corrections are shown in Fig. 1. The relevant Feynman rules can be found in Ref. [1]. In our calculation, we use dimensional regularization to regulate all the ultraviolet divergences in the virtual loop corrections and we adopt the on-mass-shell renormalization scheme [12]. We work in the approximation of negligible squark mixing and electron mass. Note that in the renormalized amplitude given in this paper, we only take into account the SUSY $O(\alpha m_t^2/m_W^2)$ corrections arising from chargino, neutralino, and squark loops, not including the SM corrections, the two Higgs doublet model (2HDM) corrections and the SUSY $O(\alpha_s)$ corrections which have been well known.

Taking into account the SUSY $O(\alpha m_t^2/m_W^2)$ corrections, the renormalized amplitude for $e^+e^- \to t\bar{t}$ is given by

$$M_{\rm ren} = M_0 + \delta M^{(\gamma)} + \delta M^{(Z)} + \delta M_{\rm box} , \tag{2.1}$$

where M_0 is the amplitude at tree level, $\delta M^{(\gamma,Z)}$ and $\delta M_{\rm box}$ represent the SUSY $O(\alpha m_t^2/m_W^2)$ corrections arising from the effective $\gamma t\bar{t}(Zt\bar{t})$ vertex and box diagrams, respectively. $\delta M^{(\gamma,Z)}$ are given by

$$\delta M^{(\gamma)} = \bar{v}(p_+,\kappa_+)V^{\nu}_{\gamma ee}u(p_-,\kappa_-)D^{\gamma}_{\mu\nu}\bar{u}(p_t,\eta)\delta V^{\mu}_{\gamma t\bar{t}}v(p_{\bar{t}},\bar{\eta}) , \tag{2.2}$$

$$\delta M^{(Z)} = \bar{v}(p_+,\kappa_+)V^{\nu}_{Zee}u(p_-,\kappa_-)D^{Z}_{\mu\nu}\bar{u}(p_t,\eta)\delta V^{\mu}_{Zt\bar{t}}v(p_{\bar{t}},\bar{\eta}) , \tag{2.3}$$

where, p_- (p_+), κ_- (κ_+) denote the momentum and helicity of the incoming electron (positron), and, correspondingly, p_t ($p_{\bar{t}}$), η ($\bar{\eta}$) are used for the outgoing t quark and its antiparticle. The values + and − of the variables κ and η refer to helicities $+\frac{1}{2}$ and $-\frac{1}{2}$, respectively. $V^{\nu}_{\gamma ee}$ and V^{ν}_{Zee} are the tree-level vertex for photon-electron-positron and Z-boson–electron–positron interactions, respectively. $D^{\gamma,Z}_{\mu\nu}$ denotes the photon (Z-boson) propagator. $\delta V^{\mu}_{\gamma t\bar{t}}$, $\delta V^{\mu}_{Zt\bar{t}}$ stand for the SUSY $O(\alpha m_t^2/m_W^2)$ corrections to $\gamma t\bar{t}$ and $Zt\bar{t}$ vertex, respectively, which are given by

$$\delta V^{\mu}_{\gamma t\bar{t},Zt\bar{t}} = -i\left(\gamma^{\mu}F_1^{(\gamma,Z)} + \gamma^{\mu}\gamma_5 F_2^{(\gamma,Z)} + k^{\mu}F_3^{(\gamma,Z)} + k^{\mu}\gamma_5 F_4^{(\gamma,Z)} + ik_{\nu}\sigma^{\mu\nu}F_5^{(\gamma,Z)} + ik_{\nu}\sigma^{\mu\nu}\gamma_5 F_6^{(\gamma,Z)}\right) , \tag{2.4}$$

where $\sigma^{\mu\nu} = (i/2)[\gamma^{\mu},\gamma^{\nu}]$ and $F_i^{(\gamma,Z)}$ are form factors which are presented in Appendix A.

The calculation of box diagrams results in

$$\delta M_{\rm box} = \delta M^{11}_{\rm box} + \delta M^{12}_{\rm box} + \delta M^{21}_{\rm box} + \delta M^{22}_{\rm box} , \tag{2.5}$$

$$\begin{aligned}\delta M^{11}_{\rm box} = -i[&\bar{u}(p_t,\eta)P_L u(p_-,\kappa_-)\bar{v}(p_+,\kappa_+)P_R v(p_{\bar{t}},\bar{\eta})f_1^{11} + \bar{u}(p_t,\eta)P_L u(p_-,\kappa_-)\bar{v}(p_+,\kappa_+)P_R\gamma_{\mu}p_t^{\mu}v(p_{\bar{t}},\bar{\eta})f_2^{11}\\ &+\bar{u}(p_t,\eta)P_R\gamma_{\mu}p_{\bar{t}}^{\mu}u(p_-,\kappa_-)\bar{v}(p_+,\kappa_+)P_R v(p_{\bar{t}},\bar{\eta})f_3^{11} + \bar{u}(p_t,\eta)P_R\gamma_{\mu}P_{\bar{t}}^{\mu}u(p_-,\kappa_-)\bar{v}(p_+,\kappa_+)P_R\gamma_{\mu}p_t^{\mu}v(p_{\bar{t}},\bar{\eta})f_4^{11}\\ &+\bar{u}(p_t,\eta)P_R\gamma_{\mu}u(p_-,\kappa_-)\bar{v}(p_+,\kappa_+)P_R\gamma^{\mu}v(p_{\bar{t}},\bar{\eta})f_5^{11}] ,\end{aligned} \tag{2.6}$$

$$\delta M^{12}_{\rm box} = \delta M^{11}_{\rm box}|_{f_i^{11}\to f_i^{12}}, \tag{2.7}$$

$$\delta M^{21}_{\rm box} = \delta M^{11}_{\rm box}|_{P_{L,R}\to P_{R,L},f_i^{11}\to f_i^{21}}, \tag{2.8}$$

$$\delta M^{22}_{\rm box} = \delta M^{21}_{\rm box}|_{f_i^{21}\to f_i^{22}}. \tag{2.9}$$

The form factors $f_i^{\alpha\beta}$ are presented in Appendix A.

Using the definition and the unitary property of the matrices U, V, and N, we found through simple calculation that all the ultraviolet divergences have canceled in the renormalized amplitude, as they should.

In the limit $m_e/E \to 0$, we can write the renormalized differential cross section as

$$\frac{d\sigma}{d\cos\theta}(s,\cos\theta) = -\sum_{\kappa=\pm}\tfrac{1}{4}(1+\kappa P_{e^-})(1-\kappa P_{e^+})\frac{N_c}{32\pi s}\sqrt{1-4m_t^2/s}\sum_{\eta,\bar{\eta}=\pm}|M_{\rm ren}|^2 , \tag{2.10}$$

where $\kappa = \kappa_{e^-} = -\kappa_{e^+}$, and P_{e^-}, P_{e^+} denote the degrees of polarization of the electron and positron beam, respectively. Purely left-handed, right-handed, or unpolarized electrons (positrons) correspond to P_{e^-} $(P_{e^+}) = -1, +1, 0$, respectively. θ is the angle between top quark and electron. The squared matrix element for left-handed and right-handed polarized electrons are obtained by

$$|M_{\rm ren}|^2_{L,R} = |M_0|^2_{L,R} + \delta|M|^2_{L,R} , \tag{2.11}$$

$$|M_0|^2_{L,R} = \sum_{\eta,\bar{\eta}=\pm}|M_0^{(\gamma)} + M_0^{(Z)}|^2_{\kappa=-,+} , \tag{2.12}$$

$$\delta|M|^2_{L,R} = \sum_{\eta,\bar{\eta}=\pm} 2\,{\rm Re}[(\delta M^{(\gamma)} + \delta M^{(Z)} + \delta M_{\rm box})(M_0^{(\gamma)} + M_0^{(Z)})^{\dagger}]|_{\kappa=-,+} . \tag{2.13}$$

The expressions for these squared matrix elements are given in Appendix B.

The forward-backward and left-right asymmetries are defined as

$$A_{\rm FB}(s) = \frac{\sigma^F(s) - \sigma^B(s)}{\sigma^F(s) + \sigma^B(s)} , \tag{2.14}$$

$$A_{\rm LR}(s) = \frac{\sigma^L(s) - \sigma^R(s)}{\sigma^L(s) + \sigma^R(s)} . \tag{2.15}$$

Here $\sigma^F(s)$ and $\sigma^B(s)$ stand for the cross section in forward and backward directions, respectively. $\sigma^L(s)$ and $\sigma^R(s)$ stand for the cross section for left-handed and right-handed electrons, respectively.

In our numerical results we present the quantities σ/σ_0, $\delta A_{\rm FB}$, and $\delta A_{\rm LR}$ which are defined as

$$\sigma/\sigma_0 = 1 + \delta\sigma^{\rm SUSY}/\sigma_0 , \tag{2.16}$$

$$\delta A_{\rm FB} = A_{\rm FB}^{\rm SUSY} - A_{\rm FB}^0 , \tag{2.17}$$

$$\delta A_{\rm LR} = A_{\rm LR}^{\rm SUSY} - A_{\rm LR}^0 , \tag{2.18}$$

where σ_0, $A_{\rm FB}^0$, and $A_{\rm LR}^0$ stand for the values in the Born approximation while $\sigma^{\rm SUSY}$, $A_{\rm FB}^{\rm SUSY}$, and $A_{\rm LR}^{\rm SUSY}$ refer to the values with SUSY $O(\alpha m_t^2/m_W^2)$ corrections.

III. CALCULATIONS FOR $b\bar{b}$ PRODUCTION

The Feynman diagrams are shown in Fig. 2. The relevant Feynman rules can be found in Ref. [1]. The renormalized amplitudes take the same form as in Eq. (2.1), with $\delta M^{(\gamma,Z)}$ and $\delta M_{\rm box}$ given by

$$\delta M^{(\gamma)} = i\frac{e^2}{3s}F^{(\gamma)}\bar{v}(p_+,\kappa_+)\gamma_\mu u(p_-,\kappa_-)\bar{u}(p_b,\eta)\gamma^\mu P_L v(p_{\bar{b}},\bar{\eta}) \ , \tag{3.1}$$

$$\delta M^{(Z)} = i\frac{e^2}{s-m_Z^2}F^{(Z)}\bar{v}(p_+,\kappa_+)\gamma_\mu(v_e-a_e\gamma_5)u(p_-,\kappa_-)\bar{u}(p_b,\eta)\gamma^\mu P_L v(p_{\bar{b}},\bar{\eta}) \ , \tag{3.2}$$

$$\delta M_{\rm box} = i[F_1^{\rm box}p_{\bar{b}\mu}p_{b\nu} - F_2^{\rm box}p_{+\mu}p_{b\nu} - F_3^{\rm box}g_{\mu\nu}]\bar{u}(p_b,\eta)\gamma^\mu P_L u(p_-,\kappa_-)\bar{v}(p_+,\kappa_+)P_R\gamma^\nu v(p_{\bar{b}},\bar{\eta}) \ . \tag{3.3}$$

Here v_e and a_e are the vector and axial-vector coupling constants of electron to the Z boson. $\sqrt{s}$ is the center-of-mass energy. $p_b(p_{\bar{b}}),\eta(\bar{\eta})$ denote the momentum and helicity of the outgoing b quark and its antiparticle. The form factors $F^{(Z)}$, $F^{(\gamma)}$ are given by

$$F^{(Z)} = \frac{\alpha}{2\pi}\frac{m_t^2}{m_W^2\sin^2\beta}[F_1^{(Z)}+F_2^{(Z)}+F_3^{(Z)}+F_4^{(Z)}+F_5^{(Z)}] \ , \tag{3.4}$$

$$F^{(\gamma)} = -\frac{3\alpha}{4\pi}\frac{m_t^2}{m_W^2\sin^2\beta}[F_1^{(\gamma)}+F_2^{(\gamma)}+F_3^{(\gamma)}+F_4^{(\gamma)}+F_5^{(\gamma)}] \ , \tag{3.5}$$

with

$$F_1^{(Z)} = \frac{v_b+a_b}{2s_W^2}[\cos^2\beta B_1(m_b,m_t,m_{H^+}) + \sum_{i=1,2}|V_{i2}|^2 B_1(m_b,\tilde{M}_i,\tilde{m}_t)] \ , \tag{3.6}$$

$$F_2^{(Z)} = \frac{v_t-a_t}{4s_W^2}\cos^2\beta[4c_{24}-2s(c_{23}-c_{22})-1] - \frac{v_t+a_t}{2s_W^2}\cos^2\beta m_t^2 c_0(p_b,-p_b-p_{\bar{b}},m_H+,m_t,m_t) \ , \tag{3.7}$$

$$F_3^{(Z)} = -\frac{\cos 2\theta_W}{2s_W^3 c_W}\cos^2\beta c_{24}(-p_b,p_b+p_{\bar{b}},m_t,m_{H^+},m_{H^+}) \ , \tag{3.8}$$

$$F_4^{(Z)} = -\frac{2}{3s_W c_W}|V_{i2}|^2 c_{24}(-p_b,p_b+p_{\bar{b}},\tilde{M}_i,\tilde{m}_t,\tilde{m}_t) \ , \tag{3.9}$$

$$F_5^{(Z)} = \frac{1}{4s_W^3 c_W}\sum_{i,j=1,2}V_{i2}^*V_{j2}[O_{ij}'^L(4c_{24}-2sc_{23}+2sc_{22}-1) - 2O_{ij}'^R\tilde{M}_i\tilde{M}_j c_0](-p_b,p_b+p_{\bar{b}},\tilde{M}_i,\tilde{m}_t,\tilde{M}_j,\tilde{M}_i) \ , \tag{3.10}$$

$$F_1^{(\gamma)} = F_1^{(Z)}|_{a_b\to 0,v_b\to -1/3}, \quad F_2^{(\gamma)} = F_2^{(Z)}|_{a_t\to 0,v_t\to 2/3} \ , \tag{3.11}$$

$$F_3^{(\gamma)} = F_3^{(Z)}|_{\cos 2\theta_W\to\sin 2\theta_W}, \quad F_4^{(\gamma)} = -\frac{c_W}{s_W}F_4^{(Z)} \ , \tag{3.12}$$

$$F_5^{(\gamma)} = -c_W s_W \delta_{ij}F_5^{(Z)}|_{O_{ij}'^L\to 1,O_{ij}'^R\to 1} \ , \tag{3.13}$$

and $F_{1,2,3}^{\rm box}$ are given by

$$F_{1,2,3}^{\rm box} = \frac{g^4}{32\pi^2}\frac{m_t^2}{m_W^2\sin^2\beta}V_{i1}V_{j1}^*V_{i2}^*V_{j2}[(D_{12}+D_{24}),(D_{13}+D_{25}),D_{27}] \ . \tag{3.14}$$

In the above, $s_W \equiv \sin\theta_W$ and $c_W \equiv \cos\theta_W$, $v_b(v_t)$, $a_b(a_t)$ are the vector and axial-vector coupling constants of the bottom (top) quark to the Z boson. The functions $B_{0,1}$, c_0, c_{ij}, and $D_{ij}(-p_b, -p_{\bar{b}}, p_+, \tilde{M}_j, \tilde{m}_t, \tilde{M}_i, \tilde{M}_\nu)$ in Eq. (3.14) are the Feynman integrals, definition and expression for which can be found in Ref. [13]. $O_{ij}^{\prime L,R}$, the chargino mass $\tilde{M}_j$ as well as the matrix elements U_{ij} and V_{ij} can be found in Ref. [1]. M, μ are the soft SUSY-breaking parameters, which can vary in a large range [11].

The renormalized differential cross section takes the same form as in Eq. (2.10), with squared matrix elements for left-handed and right-handed polarized electrons given by

$$|M_0|^2_{L,R} = \frac{4e^4}{9s^2}(u^2+t^2) + \frac{4e^4}{(s-m_Z^2)^2}(v_e \pm a_e)^2[(v_b \pm a_b)^2u^2 + (v_b \mp a_b)^2t^2] + \frac{8e^4}{3s(s-m_Z^2)}(v_e \pm a_e)[(v_b \pm a_b)u^2 + (v_b \mp a_b)t^2] , \tag{3.15}$$

$$\delta|M|^2_L = \frac{8e^4}{(s-m_Z^2)^2}F^{(Z)}(v_e+a_e)^2(v_b+a_b)u^2 + \frac{8e^4}{3s(s-m_Z^2)}(v_e+a_e)u^2[F^{(Z)}+F^{(\gamma)}(v_b+a_b)] + \frac{8e^4}{9s^2}F^{(\gamma)}u^2 + \left[\frac{2e^2}{3s} + \frac{2e^2}{s-m_Z^2}(v_e+a_e)(v_b+a_b)\right][2F_1^{\rm box}su^2 - F_2^{\rm box}u(u^2+s^2-t^2) - 4F_3^{\rm box}u^2] , \tag{3.16}$$

$$\delta|M|^2_R = \frac{8e^4}{(s-m_Z^2)^2}F^{(Z)}(v_e-a_e)^2(v_b+a_b)t^2 + \frac{8e^4}{9s^2}F^{(\gamma)}t^2 + \frac{8e^4}{3s(s-m_Z^2)}(v_e-a_e)t^2[F^{(Z)}+F^{(\gamma)}(v_b+a_b)] , \tag{3.17}$$

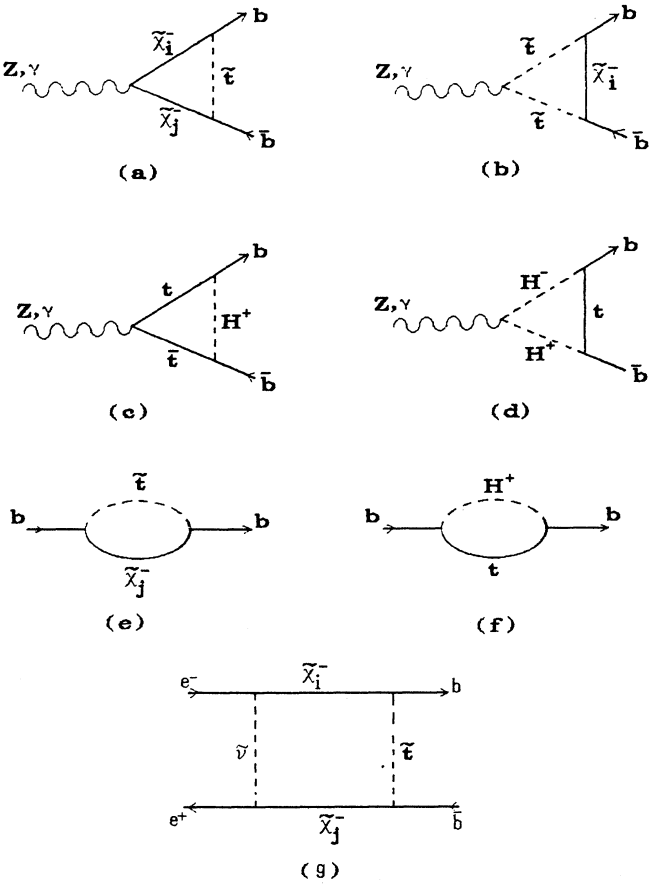

FIG. 2. Feynman diagrams contributing to $O(\alpha m_t^2/m_W^2)$ corrections to $e^+e^- \to b\bar{b}$, where $\tilde{\nu}$, H^+ stand for scalar neutrino and charged Higgs boson, respectively.

where s, t, u are the Mandelstam variables which are defined by

$$\begin{aligned} s &= (p_- + p_+)^2 = (p_b + p_{\bar{b}})^2 , \\ t &= (p_- - p_b)^2 = (p_+ - p_{\bar{b}})^2 , \\ u &= (p_- - p_{\bar{b}})^2 = (p_+ - p_b)^2 . \end{aligned} \tag{3.18}$$

The definitions for forward-backward, left-right asymmetries, and the quantities $\delta\sigma, \delta A_{\rm FB}, \delta A_{\rm LR}$ are the same as in $e^+e^- \to t\bar{t}$ case.

IV. NUMERICAL RESULTS AND CONCLUSIONS

In the numerical results presented in Figs. 3–11, for simplicity, we only consider the case of unmixed top squarks, i.e., the mixing angle between the left- and right-handed top squarks $\theta = 0$, and assume the degeneration between the two mass eigenstates of each squark. If we consider the mixing between the left- and right-handed squarks, i.e., keep the mixing angle θ as a new variable, the corrections will be slightly larger or smaller, depending on the value of θ. The scalar electron mass, scalar neutrino mass and the parameters M, μ are fixed to be 100, 150, 200, and -100 GeV, respectively. Other input parameters are [14] $m_Z = 91.176$ GeV, $\alpha_{\rm em} = 1/128.8$, and $G_F = 1.166\,372 \times 10^{-5}$ (GeV)$^{-2}$. m_W is determined through [15]

$$m_W^2\left(1 - \frac{m_W^2}{M_Z^2}\right) = \frac{\pi\alpha}{\sqrt{2}G_F}\frac{1}{1-\Delta r} , \tag{4.1}$$

where Δr depends on all parameters of the model, especially on the mass of the top squark. Since the ad-

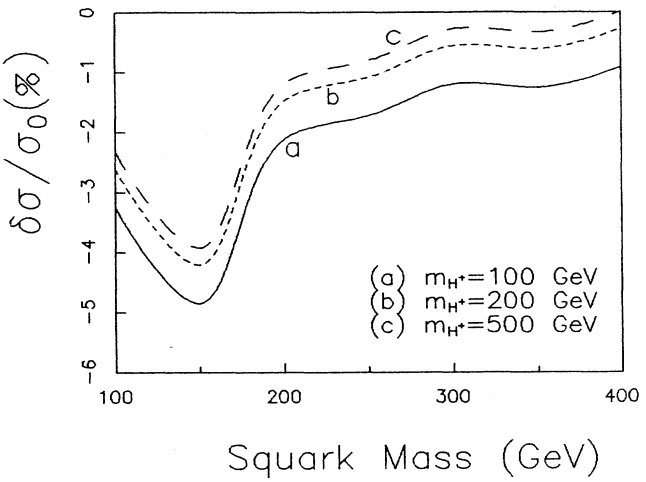

FIG. 3. Plot of $\delta\sigma/\sigma_0$ for $b\bar{b}$ production vs top squark mass with $m_t = 170$ GeV, $\sqrt{s} = 500$ GeV, $\tan\beta = 1$ and different charged Higgs boson masses.

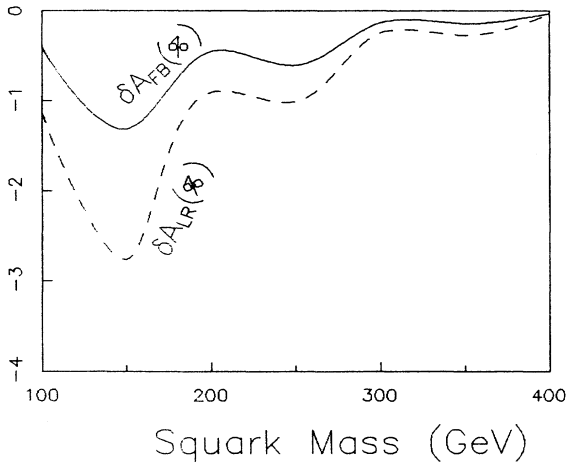

FIG. 4. Same as Fig. 3, but for plots $\delta A_{\rm FB}$ and $\delta A_{\rm LR}$ with $m_{H^+} = 500$ GeV.

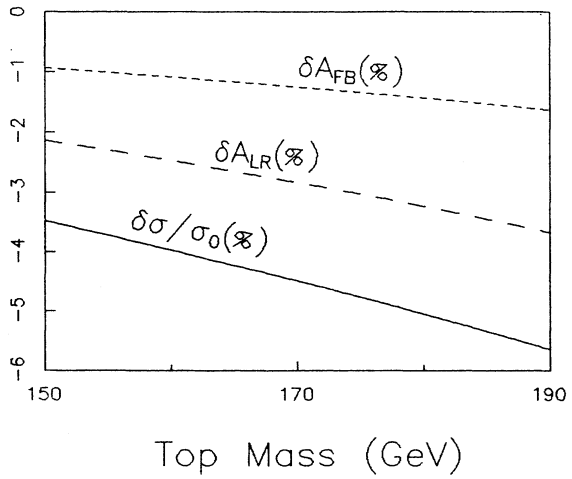

FIG. 5. Plots of $\delta\sigma/\sigma_0$, $\delta A_{\rm FB}$, and $\delta A_{\rm LR}$ for $b\bar{b}$ production vs top quark mass with $\sqrt{s} = 500$ GeV, $\tilde{m}_t = m_{H^+} = 150$ GeV and $\tan\beta = 1$.

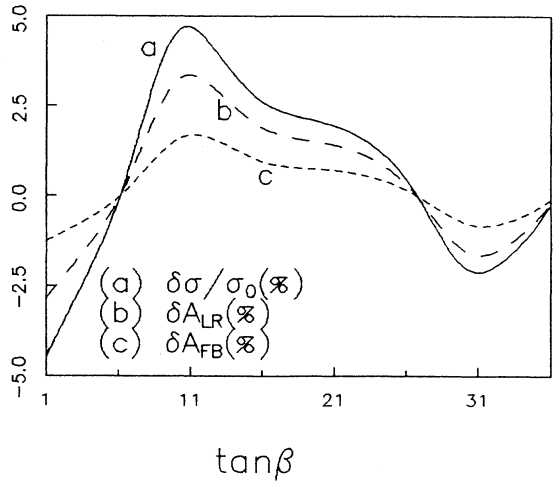

FIG. 6. Same as Fig. 5, but vs $\tan\beta$ with $\sqrt{s} = 500$ GeV, $m_t = 170$ GeV, $\tilde{m}_t = m_{H^+} = 150$ GeV.

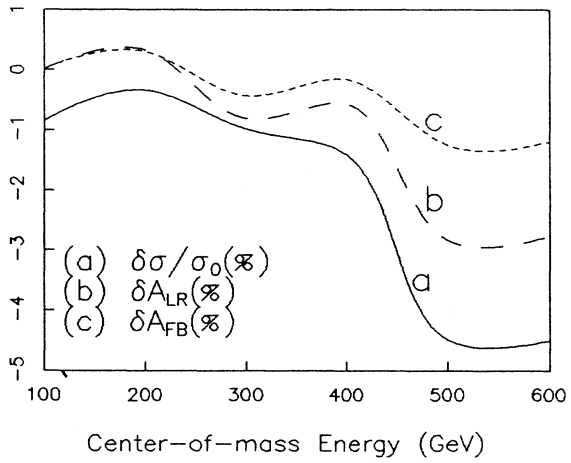

FIG. 7. Same as Fig. 5, but vs center-of-mass energy $\sqrt{s}$ for $m_t = 170$ GeV, $\tilde{m}_t = m_{H^+} = 150$ GeV, and $\tan\beta = 1$.

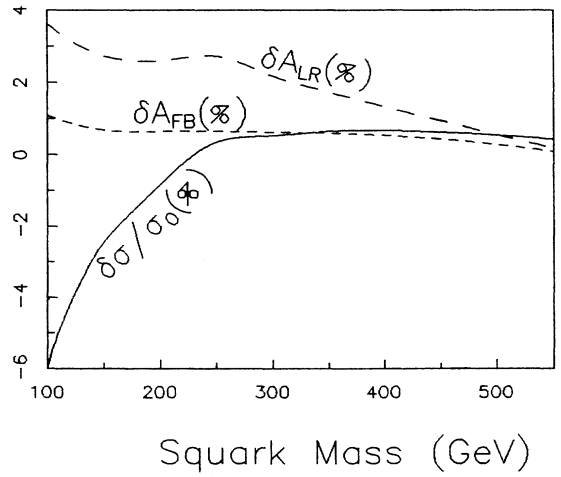

FIG. 8. Plot of $\delta\sigma/\sigma_0$, $\delta A_{\rm FB}$ and $\delta A_{\rm LR}$ for $t\bar{t}$ production vs squark mass for $\sqrt{s} = 500$ GeV, $m_t = 170$ GeV, and $\tan\beta = 1$.

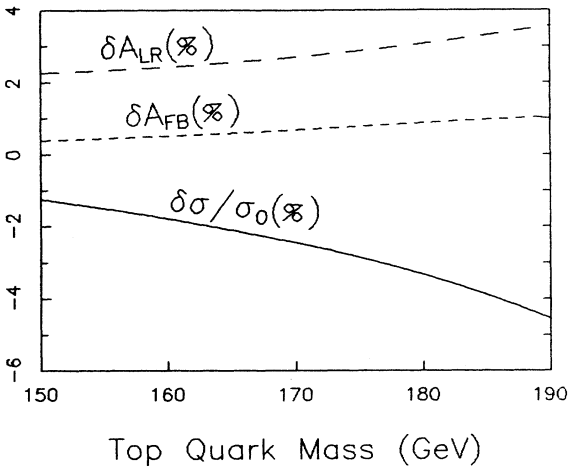

FIG. 9. Same as Fig. 8, but vs top quark mass for squark mass $\tilde{m}_q = 150$ GeV.

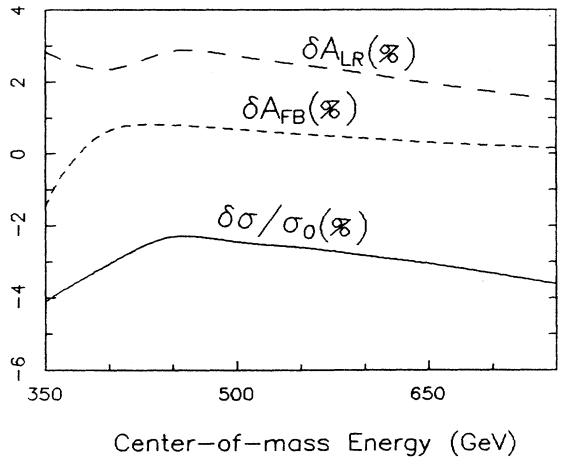

FIG. 10. Same as Fig. 8, but vs center-of-mass energy for $\tilde{m}_q = 150$ GeV.

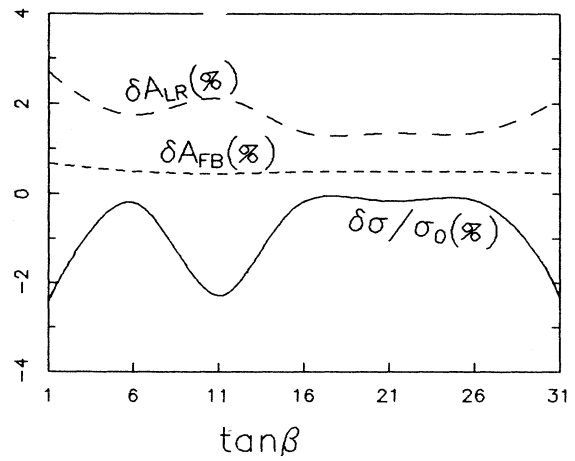

FIG. 11. Same as Fig. 8, but vs tanβ for $\tilde{m}_q = 150$ GeV.

ditional contributions to Δr in the MSSM contain no $O(\alpha m_t^2/m_W^2)$ terms, Δr is given by [16]

$$\Delta r \sim -\frac{\alpha N_C c_W^2 m_t^2}{16\pi^2 s_W^4 m_W^2}\ , \tag{4.2}$$

for a heavy top quark.

In our numerical results we will discuss the dependence on the masses of squarks and charged Higgs bosons. The CDF limit [17] on the squark mass without cascade decays is $\tilde{m}_q > 126$ GeV when the gluino mass is large, but when cascade decays are considered, there are no limits for the squark mass when the gluino mass is larger than 410 GeV. The charged Higgs boson in the MSSM is heavier than the W boson due to the relation $m_{H^\pm} = m_W^2 + m_A^2$ [18]. The latest experimental bound of $B(b \to s\gamma)$ seems to set a much stricter lower bound (> 100 GeV) for charged Higgs boson mass [19].

For $b\bar{b}$ production, some numerical results are presented in Figs. 3–7. Figure 3 shows the dependence of the correction of the cross section on the top squark mass $\tilde{m}_t$ and charged Higgs boson mass m_{H^+}. The correction obtains its maximum size at $\tilde{m}_t = 150$ GeV and then decreases rapidly as $\tilde{m}_t$ grows. It also decreases with m_{H^+}. When $m_{H^+} > 400$ GeV, the contribution of the charged Higgs couplings vanishes and thus the corrections arise only from the chargino couplings. In Fig. 4, the dependences of $\delta A_{\rm FB}$ and $\delta A_{\rm LR}$ on the top squark mass are shown with $m_{H^+} = 500$ GeV. Even for a large enough charged Higgs boson mass, we see from Figs. 3 and 4 that both $\delta\sigma$ and $\delta A_{\rm LR}$ can be up to a few percent for $\tilde{m}_t < 200$ GeV. As shown in Fig. 5, such SUSY $O(\alpha m_t^2/m_W^2)$ corrections grow with top quark mass. Since the charged Higgs coupling, the chargino masses as well as the matrix elements U_{ij} and V_{ij} are all dependent on tanβ, the corrections will depend strongly on tanβ. In Fig. 6, we present the dependence on tanβ. The dependence on the center-of-mass energy $\sqrt{s}$ is given in Fig. 7. For $\sqrt{s} < 400$ GeV the corrections are small, only $\delta\sigma$ can reach $\sim 1\%$. But for $\sqrt{s} = 500$ GeV the corrections can reach a few percent.

As presented in Ref. [10], the SUSY QCD correction to the $b\bar{b}$ production cross section can reach +2% for favorable parameter values, but the correction to the forward-backward asymmetry is very small ($< 0.1\%$). The SUSY $O(\alpha m_t^2/m_W^2)$ corrections presented above combined with the SUSY QCD correction [10] constitutes the dominant part of the one-loop SUSY correction to $b\bar{b}$ production above the Z resonance, which can reach a few percent for favorable parameter values. In the SM the QCD correction can be approximately obtained through the substitution given by Eq. (24) in the second reference of Ref. [10], which reaches a few percent. In Ref. [6], Lynn and Stuart presented the electroweak corrections in a compact form in terms of the Feynman integral functions, in which they considered the Z exchange diagram, the photon exchange diagram as well as the box diagram, but did not provide the numerical results.

For $t\bar{t}$ production, we present some numerical examples in Figs. 8–11. In Fig. 8, we present the corrections to the total cross section, to forward-backward asymmetry, and to left-right asymmetry versus squark mass

($\tilde{m}_q = \tilde{m}_t = \tilde{m}_b$). This figure shows that the corrections depend strongly on the squark mass, decreasing with the squark mass. The correction to left-right asymmetry can be larger than 1% for $\tilde{m}_q \leq 400$ GeV and the correction to the cross section can also be larger than 1% for $\tilde{m}_q \leq 200$ GeV. For example, when $\tilde{m}_q = 150$ GeV the corrections to the cross section and to left-right asymmetry are about -3 and $+3\%$, respectively. But the correction to the forward-backward asymmetry is negligibly small, reaching the 1% level only for $\tilde{m}_q \leq 100$ GeV. The dependence on top quark mass is shown in Fig. 9. Such SUSY $O(\alpha m_t^2/m_W^2)$ corrections grow with top quark mass as they should. The dependence on center-of-mass energy $\sqrt{s}$ is given in Fig. 10. In Fig. 11, we present the corrections versus $\tan\beta$.

Now we compare these genuine SUSY $O(\alpha m_t^2/m_W^2)$ corrections to $t\bar{t}$ production with the extra Higgs contribution, the SUSY QCD correction as well as the SM corrections. The extra Higgs contribution [9] can be either positive or negative, depending on the parameter values. For a light pseudoscalar, the magnitude of the extra Higgs contribution can reach 4% for the cross section and 2% for left-right asymmetry, but cannot reach the 1% level for forward-backward asymmetry. As presented in the second reference of Ref. [10], the SUSY QCD corrections to the cross section and forward-backward asymmetry for $t\bar{t}$ production at NLC cannot reach the 1% level. The genuine SUSY $O(\alpha m_t^2/m_W^2)$ corrections combined with the extra Higgs boson contribution [9] as well as the SUSY QCD corrections [10] constitute the dominant part of the SUSY correction to top quark pair production in e^+e^- annihilation. The total effects can be up to a few percent, which are comparable to the SM electroweak correction ($\sim -6\%$) [7] and the QCD correction ($\sim +10\%$) [8] in the SM.

Since it is possible to measure all of the various production and decay form factors of the top quark at the level of a few percent at NLC [5], such SUSY effects might be detectable at the NLC. If any deviation from the SM prediction is detected in top quark pair production at NLC, these virtual effects of genuine supersymmetric particles might allow one to confirm its interpretation in terms of SUSY.

In conclusion, we have calculated the SUSY $O(\alpha m_t^2/m_W^2)$ corrections to $t\bar{t}$ and $b\bar{b}$ production in e^+e^- annihilation in the minimal supersymmetric model. The corrections to total cross-section and left-right asymmetry can both be up to a few percent for favorable values of the parameters and thus might be detectable at the next-generation linear collider if SUSY exists.

APPENDIX A

Here we present the form factors appearing in Sec. II for $t\bar{t}$ production process. The form factors $F_i^{(\gamma,Z)}$ in the vertex corrections are

$$F_1^{(\gamma,Z)} = \tfrac{1}{2}[Y_0^{\gamma,Z} + Y_1^{\gamma,Z} + m_t(Y_2^{\gamma,Z} + Y_3^{\gamma,Z} - Y_4^{\gamma,Z} - Y_5^{\gamma,Z})] , \tag{A1}$$

$$F_2^{(\gamma,Z)} = \tfrac{1}{2}[Y_1^{\gamma,Z} - Y_0^{\gamma,Z}] , \tag{A2}$$

$$F_3^{(\gamma,Z)} = \tfrac{1}{4}[Y_2^{\gamma,Z} + Y_3^{\gamma,Z} + Y_4^{\gamma,Z} + Y_5^{\gamma,Z}] , \tag{A3}$$

$$F_4^{(\gamma,Z)} = \tfrac{1}{4}[Y_2^{\gamma,Z} + Y_4^{\gamma,Z} - Y_3^{\gamma,Z} - Y_5^{\gamma,Z}] , \tag{A4}$$

$$F_5^{(\gamma,Z)} = \tfrac{1}{4}[Y_4^{\gamma,Z} + Y_5^{\gamma,Z} - Y_2^{\gamma,Z} - Y_3^{\gamma,Z}] , \tag{A5}$$

$$F_6^{(\gamma,Z)} = \tfrac{1}{4}[Y_3^{\gamma,Z} + Y_4^{\gamma,Z} - Y_2^{\gamma,Z} - Y_5^{\gamma,Z}] , \tag{A6}$$

where $Y^{\gamma Z}$ are given by

$$Y_\alpha^{\gamma,Z} = \sum_{\beta=1}^{3} T_{\beta\alpha}^{\gamma,Z} + \sum_{\beta=1}^{5} S_{\beta\alpha}^{\gamma,Z} . \tag{A7}$$

From the calculations of Figs. 1(a)–(f) we can write $T_{\beta\alpha}^{\gamma,Z}$ as

$$T_{11}^Z = -2\xi_{jj}(\tfrac{1}{2} - \tfrac{1}{3}s_W^2)\lambda_t^2 c_{24} , \tag{A8}$$

$$T_{12}^Z = \xi_{jj}(\tfrac{1}{2} - \tfrac{1}{3}s_W^2)\lambda_t^2 m_t(c_{12} - c_{11} - 2c_{21} - 2c_{22} + 4c_{23}) , \tag{A9}$$

$$T_{13}^Z = \xi_{jj}(\tfrac{1}{2} - \tfrac{1}{3}s_W^2)\lambda_t^2 m_t(2c_{22} - c_{12} - 2c_{23}) , \tag{A10}$$

$$T_{14}^Z = \xi_{jj}(\tfrac{1}{2} - \tfrac{1}{3}s_W^2)\lambda_t^2 m_t(c_{11} - c_{12} - 2c_{22} + 2c_{23}) , \tag{A11}$$

$$T_{15}^Z = \xi_{jj}(\tfrac{1}{2} - \tfrac{1}{3}s_W^2)\lambda_t^2 m_t(c_{12} + 2c_{22}) , \tag{A12}$$

$$T_{1i}^\gamma = T_{1i}^Z \frac{2s_W c_W}{3 - 2s_W^2} , \tag{A13}$$

$$T^Z_{20} = \xi_{ij}\lambda_t^2 O'^L_{ij} m_t^2 (c_{12} - c_{11})$$
$$+\xi'_{ij}[\tilde{M}_i \tilde{M}_j O'^L_{ij} c_0 - O'^R_{ij} m_t^2 (c_{11} + c_{12} + c_{21} + c_{22}) - O'^R_{ij}(s - 2m_t^2)(c_{12} + c_{23}) - 2O'^R_{ij} c_{24}]$$
$$-\xi''_{ij}\lambda_t m_t [\tilde{M}_j O'^L_{ij}(c_0 + c_{12}) - \tilde{M}_i O'^R_{ij} c_{12}]$$
$$-\xi'_{ji}\lambda_t m_t [\tilde{M}_j O'^R_{ij}(c_0 + c_{11}) - \tilde{M}_i O'^L_{ij} c_{11}] \ , \tag{A14}$$

$$T^Z_{21} = \xi_{ij}\lambda_t^2 [\tilde{M}_i \tilde{M}_j O'^R_{ij} c_0 - O'^L_{ij} m_t^2 (c_{11} + c_{12} + c_{21} + c_{22}) - O'^L_{ij}(s - 2m_t^2)(c_{12} + c_{23}) - 2O'^L_{ij} c_{24}]$$
$$-\xi''_{ij}\lambda_t m_t [\tilde{M}_j O'^L_{ij}(c_0 + c_{11}) - \tilde{M}_i O'^R_{ij} c_{11}]$$
$$-\xi'_{ji}\lambda_t m_t [\tilde{M}_j O'^R_{ij}(c_0 + c_{12}) - \tilde{M}_i O'^L_{ij} c_{12}] + \xi'_{ij} O'^R_{ij} m_t^2 (c_{12} - c_{11}) \ , \tag{A15}$$

$$T^Z_{22} = 2\xi_{ij}\lambda_t^2 O'^L_{ij} m_t (c_{12} + c_{22}) \ , \tag{A16}$$

$$T^Z_{23} = -T^Z_{24} = -2\xi_{ij}\lambda_t^2 O'^L_{ij} m_t (c_{12} + c_{23}) \ , \tag{A17}$$

$$T^Z_{25} = -2\xi_{ij}\lambda_t^2 O'^L_{ij} m_t (c_{11} + c_{21}) \ , \tag{A18}$$

$$T^\gamma_{2\alpha} = -T^Z_{2\alpha} s_W c_W \delta_{ij} | O'^L_{ij} \to 1, O'^R_{ij} \to 1 \ , \tag{A19}$$

$$T^Z_{30} = \frac{g^2}{16\pi^2} e(v_t + a_t)[m_t^2 (U_{j1}^2 + \lambda_t^2 V_{j2}^2)\partial B_1(p, \tilde{M}_j, \tilde{m}_b)/\partial p^2 + 2m_t \lambda_t \tilde{M}_j U_{j1} V_{j2} \partial B_0(p, \tilde{M}_j, \tilde{m}_b)/\partial p^2]|_{p^2 = m_t^2} \ , \tag{A20}$$

$$T^Z_{31} = \frac{g^2}{16\pi^2} e(v_t - a_t)[\lambda_t^2 V_{j2}^2 B_1(p, \tilde{M}_j, \tilde{m}_b) + m_t^2 (U_{j1}^2 + \lambda_t^2 V_{j2}^2)\partial B_1(p, \tilde{M}_j, \tilde{m}_b)/\partial p^2$$
$$+2m_t \lambda_t \tilde{M}_j U_{j1} V_{j2} \partial B_0(p, \tilde{M}_j, \tilde{m}_b)/\partial p^2]|_{p^2 = m_t^2} \ , \tag{A21}$$

$$(T^\gamma_{30}, T^\gamma_{31}) = (T^Z_{30}, T^Z_{31})|_{a_t \to 0, v_1 \to 2/3} \ , \tag{A22}$$

where, v_t, a_t are the vector and axial-vector coupling constants of the top quark to the Z boson, and

$$\xi_{ij} = \frac{g^2}{16\pi^2} \frac{e}{s_W c_W} V^*_{i2} V_{j2} \ , \tag{A23}$$

$$\xi'_{ij} = \xi_{ij}|_{V_{i2} \to U^*_{i1}, V_{j2} \to U^*_{j1}}, \quad \xi''_{ij} = \xi_{ij}|_{V_{j2} \to U_{j1}} \ , \tag{A24}$$

$$\lambda_t = \frac{m_t}{\sqrt{2} m_W \sin\beta} \ . \tag{A25}$$

$S^{\gamma Z}_{\beta\alpha}$ are given by

$$S^Z_{1\alpha} = \frac{4s_W^2 - 3}{3 - 2s_W^2} T^Z_{1\alpha}|_{U_{j1} \to L_j, V_{j2} \to N_{j4}, \tilde{M}_j \to \tilde{M}_{0j}, \tilde{m}_b \to \tilde{m}_t} \ , \tag{A26}$$

$$(S^Z_{20}, S^Z_{22}, S^Z_{23}, S^Z_{24}, S^Z_{25}) = \frac{4s_W^2}{4s_W^2 - 3}(S^Z_{11}, S^Z_{13}, S^Z_{12}, S^Z_{15}, S^Z_{14})|_{L_j \to R_j} \ , \tag{A27}$$

$$S^Z_{3\alpha} = T^Z_{2\alpha}|_{U_{j1} \to L_j, V_{j2} \to N_{j4}, \tilde{M}_j \to \tilde{M}_{0j}, \tilde{m}_b \to \tilde{m}_t, O'^{L,R}_{ij} \to O''^{L,R}_{ij}} \ , \tag{A28}$$

$$(S^Z_{40}, S^Z_{41}, S^Z_{42}, S^Z_{43}, S^Z_{44}, S^Z_{45}) = (S^Z_{31}, S^Z_{30}, S^Z_{33}, S^Z_{32}, S^Z_{35}, S^Z_{34})|_{L_j \to R_j, O''^{L,R}_{ij} \to O''^{R,L}_{ij}} \ , \tag{A29}$$

$$S_{50}^{Z}=\frac{g^2}{16\pi^2}e(v_t+a_t)\left[\lambda_t^2N_{j4}^2B_1(p,\tilde{M}_{0j},\tilde{m}_t)+2m_t\lambda_t\tilde{M}_{0j}N_{j4}(L_j+R_j)\frac{\partial B_0(p,\tilde{M}_{0j},\tilde{m}_t)}{\partial p^2}\right.$$
$$\left.+m_t^2(2\lambda_t^2N_{j4}^2+L_j^2+R_j^2)\frac{\partial B_1(p,\tilde{M}_{0j},\tilde{m}_t)}{\partial p^2}\right]\Bigg|_{p^2=m_t^2}, \tag{A30}$$

$$S_{51}^{Z}=S_{50}^{Z}|_{a_t\to -a_t,(L_j,R_j)\to(R_j,L_j)}\ , \tag{A31}$$

$$S_{1\alpha}^{\gamma}=\frac{4s_Wc_W}{3-4s_W^2}S_{1\alpha}^{Z},\quad S_{2\alpha}^{\gamma}=-\frac{c_W}{s_W}S_{2\alpha}^{Z}\ , \tag{A32}$$

$$(S_{30}^{\gamma},S_{31}^{\gamma})=(S_{50}^{Z},S_{51}^{Z})|_{a_t\to 0,v_t\to 2/3}\ , \tag{A33}$$

where

$$L_j=-\sqrt{2}\left[\frac{2}{3}s_WN_{j1}'+\frac{1}{c_W}\left(\frac{1}{2}-\frac{2}{3}s_W^2\right)N_{j2}'\right]\ , \tag{A34}$$

$$R_j=\sqrt{2}\left(\frac{2}{3}s_WN_{j1}'^{*}-\frac{2s_W^2}{3c_W}N_{j2}'^{*}\right)\ , \tag{A35}$$

$$N_{j1}'=N_{j1}c_W+N_{j2}s_W,\quad N_{j2}'=N_{j2}c_W-N_{j1}s_W\ . \tag{A36}$$

All the other components of $T_{\beta\alpha}^{\gamma,Z}$ and $S_{\beta\alpha}^{\gamma,Z}$ which are not listed above are zero. The sums over $i,j(=1,2)$ in Eqs. (A8)–(A22) and over $i,j(=1,2,3,4)$ in Eqs. (A26)–(A33) are implied. The N_{ij} are the elements of 4×4 matrix N defined in Ref. [1] and can be calculated numerically. The neutralino mass $\tilde{M}_{0i}$ depends on the parameters M, μ, and $\tan\beta$, which can be obtained numerically. The functions $c_{ij}(-p_t,p_t+p_{\bar{t}},\tilde{M}_j,\tilde{m}_b,\tilde{m}_b)$ in Eqs. (A8)–(A13) and $c_{ij}(p_{\bar{t}},p_t,\tilde{M}_j,\tilde{m}_b,\tilde{M}_i)$ in Eqs. (A14)–(A19) are the three-point Feynman integrals, definition, and expression for which can be found in Ref. [13].

The form factors $f_i^{\alpha,\beta}$ in the box diagrams are given as

$$f_1^{11}=-\frac{g^2}{16\pi^2}E_iE_j^{*}\{A_0D_0-m_t[A_1(D_{11}-D_{13})-A_3D_{12}]-m_t^2A_2[D_{12}+D_{24}-D_{26}]\}\ , \tag{A37}$$

$$f_2^{11}=-\frac{g^2}{16\pi^2}E_iE_j^{*}\{A_1D_0+A_1D_{11}+m_tA_2(D_{12}+D_{24})\}\ , \tag{A38}$$

$$f_3^{11}=-\frac{g^2}{16\pi^2}E_iE_j^{*}\{A_3(D_{12}-D_{13})+m_t[A_2(D_{13}-D_{12}-D_{23}-D_{24}+D_{25}+D_{26})]\}\ , \tag{A39}$$

$$f_4^{11}=-\frac{g^2}{16\pi^2}E_iE_j^{*}A_2(D_{12}-D_{13}+D_{24}-D_{25})\ , \tag{A40}$$

$$f_5^{11}=-\frac{g^2}{16\pi^2}E_iE_j^{*}D_{27}\ , \tag{A41}$$

$$f_i^{12}=f_i^{11}|_{\lambda_tN_{j4}^{*}\to d_j,c_j\to\lambda_tN_{j4}}\ , \tag{A42}$$

$$f_i^{21}=f_i^{11}|_{E_{i,j}\to E_{i,j}',\lambda_tN_{j4}^{*}\to c_j,c_j\to\lambda_tN_{j4}^{*}}\ , \tag{A43}$$

$$f_i^{22}=f_i^{21}|_{\lambda_tN_{j4}\to d_j,c_j\to\lambda_tN_{j4}}\ , \tag{A44}$$

where $D_{ij}(-p_-,-p_+,p_{\bar{t}},\tilde{M}_{0j},\tilde{m}_e,\tilde{M}_{0i},\tilde{m}_t)$ are the four-point Feynman integrals, definition and expression for which can be found in Ref. [13], and

$$E_j = e\left[N'_{j1} + \frac{1}{s_W c_W}\left(\frac{1}{2} - s_W^2\right)N'_{j2}\right], \quad E'_j = e\left(N'^*_{j1} - \frac{s_W}{c_W}N'^*_{j2}\right), \tag{A45}$$

$$c_j = \sqrt{2}\left[\frac{2}{3}s_W N'_{j1} + \frac{1}{c_W}\left(\frac{1}{2} - \frac{2}{3}s_W^2\right)N'_{j2}\right], \tag{A46}$$

$$d_j = \sqrt{2}\left(\frac{2s_W^2}{3c_W}N'_{j2} - \frac{2}{3}s_W N'_{j1}\right), \tag{A47}$$

$$A_0 = \lambda_t \tilde{M}_{0j} N^*_{j4}(\lambda_t \tilde{M}_{0i} N_{i4} + m_t c_i^*), \tag{A48}$$

$$A_1 = -\lambda_t \tilde{M}_{0j} N^*_{j4} c_i^*, \quad A_2 = c_j c_i^*, \quad A_3 = -\lambda_t N_{i4} c_j . \tag{A49}$$

APPENDIX B

Here we present the expressions of the matrix elements squared for the $t\bar{t}$ production process in Sec. II. We define $G_0, G^{(Z,\gamma)}$ as

$$\begin{aligned} G_0 = {} & 2(c^e_{L0}c^e_{L1} + c^e_{R0}c^e_{R1})[(c^t_{L0}c^t_{L1} + c^t_{R0}c^t_{R1})(u^2 + t^2 - 2m_t^4 + 2m_t^2 s) + 2(c^t_{L0}c^t_{R1} + c^t_{R0}c^t_{L1})m_t^2 s] \\ & + 2(c^e_{L0}c^e_{L1} - c^e_{R0}c^e_{R1})(c^t_{L0}c^t_{L1} - c^t_{R0}c^t_{R1})s(t-u) , \end{aligned} \tag{B1}$$

$$\begin{aligned} G^{(Z,\gamma)} = {} & (c^e_{L0}c^e_{L1} + c^e_{R0}c^e_{R1})\{(c^t_{L0} + c^t_{R0})[F_1^{(Z,\gamma)}(u^2 + t^2 - 2m_t^4 + 4m_t^2 s) + 2m_t F_5^{(Z,\gamma)} s^2] \\ & - (c^t_{L0} - c^t_{R0})F_2^{(Z,\gamma)}(u^2 + t^2 - 2m_t^4)\} \\ & + (c^e_{L0}c^e_{L1} - c^e_{R0}c^e_{R1})(c^t_{L0} - c^t_{R0})s(t-u)\left[F_1^{(Z,\gamma)} - \frac{c^t_{L0} + c^t_{R0}}{c^t_{L0} - c^t_{R0}}F_2^{(Z,\gamma)} + 2m_t F_5^{(Z,\gamma)}\right], \end{aligned} \tag{B2}$$

where s, t, u are the Mandelstam variables, and

$$c^f_{L0} = c^f_{L1} = v_f - a_f, \quad c^f_{R0} = c^f_{R1} = v_f + a_f . \tag{B3}$$

Then the matrix elements squared are obtained by

$$|M_0^{(Z)}|_L^2 = \frac{e^4}{(s - m_Z^2)^2} G_0|_{c^e_{R0}\to 0} , \tag{B4}$$

$$|M_0^{(Z)}|_R^2 = \frac{e^4}{(s - m_Z^2)^2} G_0|_{c^e_{L0}\to 0} , \tag{B5}$$

$$|M_0^{(\gamma)}|_L^2 = \frac{e^4}{s^2} G_0|_{c^e_{R0}\to 0, c^e_{L0}=c^e_{L1}\to 1, c^t_{L0}=c^t_{R0}=c^t_{L1}=c^t_{R1}\to -2/3} , \tag{B6}$$

$$|M_0^{(\gamma)}|_R^2 = \frac{e^4}{s^2} G_0|_{c^e_{L0}\to 0, c^e_{R0}=c^e_{R1}\to 1, c^t_{L0}=c^t_{R0}=c^t_{L1}=c^t_{R1}\to -2/3} , \tag{B7}$$

$$M_0^{(\gamma)} M_0^{(Z)\dagger}|_R = \frac{e^4}{s(s - m_Z^2)} G_0|_{c^e_{L0}\to 0, c^e_{R0}\to 1, c^t_{L0}=c^t_{R0}\to -2/3} , \tag{B8}$$

$$M_0^{(\gamma)}M_0^{(Z)\dagger}|_L = \frac{e^4}{s(s-m_Z^2)}G_0|_{c^e_{R0}\to 0, c^e_{L0}\to 1, c^t_{L0}=c^t_{R0}\to -2/3}\ , \tag{B9}$$

$$\delta M^{(Z)}M_0^{(Z)\dagger}|_L = -\frac{2e^3}{(s-m_Z^2)^2}G^{(Z)}|_{c^e_{R0}\to 0}\ , \tag{B10}$$

$$\delta M^{(Z)}M_0^{(Z)\dagger}|_R = -\frac{2e^3}{(s-m_Z^2)^2}G^{(Z)}|_{c^e_{L0}\to 0}\ , \tag{B11}$$

$$\delta M^{(\gamma)}M_0^{(Z)\dagger}|_L = -\frac{2e^3}{s(s-m_Z^2)}G^{(\gamma)}|_{c^e_{R0}\to 0, c^e_{L1}\to 1}\ , \tag{B12}$$

$$\delta M^{(\gamma)}M_0^{(Z)\dagger}|_R = -\frac{2e^3}{s(s-m_Z^2)}G^{(\gamma)}|_{c^e_{L0}\to 0, c^e_{R1}\to 1}\ , \tag{B13}$$

$$\delta M^{(Z)}M_0^{(\gamma)\dagger}|_R = -\frac{2e^3}{s(s-m_Z^2)}G^{(Z)}|_{c^e_{L0}\to 0, c^e_{R0}\to 1, c^t_{L0}=c^t_{R0}\to -2/3}\ , \tag{B14}$$

$$\delta M^{(Z)}M_0^{(\gamma)\dagger}|_L = -\frac{2e^3}{s(s-m_Z^2)}G^{(Z)}|_{c^e_{R0}\to 0, c^e_{L0}\to 1, c^t_{L0}=c^t_{R0}\to -2/3}\ , \tag{B15}$$

$$\delta M^{(\gamma)}M_0^{(\gamma)\dagger}|_R = -\frac{2e^3}{s^2}G^{(\gamma)}|_{c^e_{L0}\to 0, c^e_{R0}=c^e_{R1}\to 1, c^t_{L0}=c^t_{R0}\to -2/3}\ , \tag{B16}$$

$$\delta M^{(\gamma)}M_0^{(\gamma)\dagger}|_L = -\frac{2e^3}{s^2}G^{(\gamma)}|_{c^e_{R0}\to 0, c^e_{L0}=c^e_{L1}\to 1, c^t_{L0}=c^t_{R0}\to -2/3}\ , \tag{B17}$$

$$\begin{aligned}\delta M_{\rm box}M_0^{(Z)\dagger}|_L = -\frac{2e^2}{s-m_Z^2}\big((f_1^{11}+f_1^{12})C_L^e[C_R^t(m_t^2-t)^2+C_L^t m_t^2 s]+(f_2^{11}+f_2^{12})m_t C_L^e[C_L^t su - C_R^t(t-m_t^2)(u-m_t^2)]\\ -(f_3^{11}+f_3^{12})m_t C_L^e[C_L^t su - C_R^t(t-m_t^2)(u-m_t^2)]-(f_4^{11}+f_4^{12})C_L^e\{C_L^t[(s-2m_t^2)(u-m_t^2)^2\\ -2m_t^2(t-m_t^2)(u-m_t^2)+m_t^4 s]+C_R^t m_t^2(u-m_t^2)^2\}-2(f_5^{11}+f_5^{12})C_L^e[C_L^t(u-m_t^2)^2+C_R^t m_t^2 s]\big)\ ,\end{aligned} \tag{B18}$$

$$\delta M_{\rm box}M_0^{(Z)\dagger}|_R = \delta M^{\rm box}M_0^{(Z)\dagger}|_L(C_L^e\to C_R^e, C_{L,R}^t\to C_{R,L}^t, f_i^{11}+f_i^{12}\to f_i^{21}+f_i^{22})\ , \tag{B19}$$

$$\delta M_{\rm box}M_0^{(\gamma)\dagger}|_L = \delta M^{\rm box}M_0^{(Z)\dagger}|_L(C_L^e\to 1, C_{L,R}^t\to -2/3, m_Z\to 0)\ , \tag{B20}$$

$$\delta M_{\rm box}M_0^{(\gamma)\dagger}|_R = \delta M^{\rm box}M_0^{(Z)\dagger}|_R(C_R^e\to 1, C_{L,R}^t\to -2/3, m_Z\to 0)\ . \tag{B21}$$

[1] H. E. Haber and G. L. Kane, Phys. Rep. **117**, 75 (1985); J. F. Gunion and H. E. Haber, Nucl. Phys. **B272**, 1 (1986).

[2] CDF Collaboration, F. Abe *et al.*, Phys. Rev. D **50**, 2966 (1994).

[3] V. Barger and R. J. N. Phillips, *Proceedings of the 7th Summer School Andre Swieca* (Particles and Fields, Sao Paulo, Brazil, 1993).

[4] A. Blondel, F. M. Renard, and C. Verzegnassi, Phys. Lett. B **269**, 419 (1991).

[5] M. E. Peskin, in *Physics and Experiments with Linear Colliders*, Proceedings of the Workshop, Saariselkä, Finland, 1991, edited by R. Orava, P. Eerola, and M. Nordberg (World Scientific, Singapore, 1992), p. 1.

[6] B. W. Lynn and R. G. Stuart, Phys. Lett. B **252**, 676 (1990).

[7] W. Beenakker, S. C. van der Marck, and W. Hollik, Nucl. Phys. **B365**, 24 (1991).

[8] P. M. Zerwas, in *Physics and Experiments with Linear Colliders* [5], p. 165; L. Reinders, H. Rubinstein, and S. Yazaki, Phys. Rep. **127**, 1 (1985); J. Schwinger, *Particles, Sources and Fields* (Addison-Wesley, Reading, MA, 1973).

[9] W. Beenakker, A. Denner, and A. Kraft, Nucl. Phys. **B410**, 219 (1993); A. Denner, R. J. Guth, and J. H. Kuhn, *ibid.* **B377**, 3 (1992).

[10] K. Hagiwara and H. Murayama, Phys. Lett. B **246**, 533 (1990); A. Djouadi, M. Drees, and H. Konig, Phys. Rev. D **48**, 3081 (1993).

[11] A. Djouadi *et al.*, Nucl. Phys. **B349**, 48 (1991); M. Boulware and D. Finnell, Phys. Rev. D **44**, 2054 (1991); C. S. Li, J. M. Yang, and B. Q. Hu, Commun. Theor. Phys. **20**, 213 (1993).

[12] K. I. Aoki *et al.*, Prog. Theor. Phys. Suppl. **73**, 1 (1982); M. Bohm, W. Hollik, H. Spiesbergerm, Fortschr. Phys. **34**, 687 (1986).

[13] A. Axelrod, Nucl. Phys. **B209**, 349 (1982); G. Passarino and M. Veltman, *ibid.* **B160**, 151 (1979); M. Clements *et al.*, Phys. Rev. D **27**, 570 (1983).

[14] Particle Data Group, K. Hikasa *et al.*, Phys. Rev. D **45**, S1 (1992).

[15] A. Sirlin, Phys. Rev. D **22**, 971 (1980); W. J. Marciano and A. Sirlin, *ibid.* **22**, 2695 (1980); **31**, 213(E) (1985); A. Sirlin and W. J. Marciano, Nucl. Phys. **B189**, 442 (1981).

[16] W. J. Marciano and Z. Parsa, Annu. Rev. Nucl. Sci. **36**, 171 (1986); W. Hollik, CERN-JINR School Physics (QCD 161) **C15**, 50, 1989 (unpublished).

[17] CDF Collaboration, Phys. Rev. Lett. **69**, 3439 (1992).

[18] J. F. Gunion, H. E. Haber, G. Kane, and S. Dawson, *The Higgs Hunters' Guide* (Addison-Wesley, Reading, MA, 1990).

[19] V. Barger, M. S. Berger, and R. J. N. Phillips, Phys. Lett. **70**, 1368 (1993); J. L. Hewett, *ibid.* **70**, 1045 (1993).